

SUSTAINABLY CHARGING BATTERIES USING COMPOST

by

Caitlin Ahearn

A senior thesis submitted to the faculty of

Ithaca College

in partial fulfillment of the requirements for the degree of

Bachelor of Science

Department of Physics

Ithaca College

April 2010

Copyright © 2010 Caitlin Ahearn

All Rights Reserved

ITHACA COLLEGE

DEPARTMENT APPROVAL

of a senior thesis submitted by

Caitlin Ahearn

This thesis has been reviewed by the research advisor, senior thesis instructor,
and department chair and has been found to be satisfactory.

Date

Michael Rogers, Advisor

Date

Matthew Price, Senior Thesis Instructor

Date

Beth Ellen Clark Joseph, Chair

ABSTRACT

SUSTAINABLY CHARGING BATTERIES USING COMPOST

Caitlin Ahearn

Department of Physics

Bachelor of Science

Fossil fuels are finite. It is estimated that peak oil production was reached in 2006. In order to avoid an energy crisis, sustainable sources of energy need to be explored. An unexpected renewable energy source is a compost pile, which produces heat energy as a byproduct of the breakdown of organic matter. Thermoelectric modules are able to take the temperature difference between hot compost and cold air and turn it into electrical current. The utilization of compost's waste energy is a step toward greener energy sources. It was previously found in laboratory replications that a compost pile is able to charge a 12 Volt battery using two thermoelectric modules. Our goal is to find the most efficient way to use thermoelectric modules to charge batteries from compost. In order to transfer the compost's energy from the hot center of the pile to the outside, different metals and insulations were tested for thermal conductivity by heating one end of an insulated metal slab and monitoring the temperatures

of both ends. Copper insulated with extruded polystyrene was found to transfer the highest percentage of energy. Maximum power output of one module held at a constant temperature difference was found by varying the resistance of an attached load and measuring voltage and current. Since maximum power output occurs at matched load, the internal resistance of the module needed to be calculated before building a charger. It was found that both the maximum power output of a module and its internal resistance increased with increasing temperature difference. Future work includes developing technology to track internal resistance in order to build an efficient thermoelectric battery charger for use with compost.

ACKNOWLEDGMENTS

The author would like to thank Professor Michael “Bodhi” Rogers, Professor Matthew C. Sullivan, Professor Bruce Thompson, and Jennifer Mellott for all their help with this project. I would also like to acknowledge the extensive work already done on this project by Colin Howard. Thanks also go to Professor Matthew Price for his help with the thesis write-up and to Professor Beth Ellen Clark Joseph for her introduction to sustainable research in the department. The author would lastly like to acknowledge the support of the Dana Internship Program at Ithaca College and the Ithaca College Physics Department.

Contents

Table of Contents	vii
List of Figures	ix
1 Introduction	1
1.1 Motivation	1
1.2 Previous Work	2
1.3 Goals	5
2 Theory	7
2.1 A Compost Pile	7
2.2 Batteries	10
2.3 Thermoelectric Modules	13
2.4 Maximum Power Point Tracking	19
3 Transferring Energy from Compost to Module	21
3.1 Methodology	21
3.2 Data and Analysis	24
3.3 Discussion	25
4 Efficient Use of Modules	27
4.1 Methodology	27
4.2 Data	30
4.2.1 First Module	30
4.2.2 Second Module	32
4.2.3 Third Module	34
4.3 Analysis	36
4.3.1 Second Module	36
4.3.2 Third Module	38
4.3.3 Error	41
4.4 Discussion	42

5	Conclusions	45
5.1	Can We Charge Batteries With Compost?	45
5.2	Future Work	46
	Bibliography	47

List of Figures

2.1	Compost windrows	8
2.2	Schematic of the inside of a battery	11
2.3	Charging curves of a NiMH battery	13
2.4	Thermoelectric module	15
2.5	Schematic of a thermocouple	16
3.1	Setup for testing metals for transfer of energy	22
3.2	Setup for testing insulations for transfer of energy	23
4.1	Setup of the module apparatus	28
4.2	First setup to test power output	30
4.3	Second setup to test power output	31
4.4	Current and voltage output of first module	32
4.5	Power output of first module	33
4.6	Current and voltage output of second module	34
4.7	Power output of second module	35
4.8	Current and voltage output of third module	36
4.9	Power output of third module	37
4.10	Maximum power of second module	38
4.11	Internal resistance of second module	39
4.12	Maximum power of third module	40
4.13	Internal resistance of third module	41

Chapter 1

Introduction

1.1 Motivation

Fossil fuels are finite. It is predicted that we have reached, or will reach very soon, international peak oil production. Peak oil was first described by Marion King Hubbert in 1956 as the point of maximum oil production and is consequently called "Hubbert's Peak." According to Hubbert, oil production follows a bell curve with the peak in the middle of the curve. Hubbert correctly predicted U.S. peak oil production which occurred in 1971, and predicted that world oil production would peak sometime between 2000 and 2010. It is currently estimated that worldwide oil production has already peaked in 2005 or 2006. After peak oil, production declines as oil is harder to discover and extract [1]. In 2006, 31 billion barrels of oil were extracted internationally but only 9 billion barrels were discovered. Additionally, the oil that is left is in dangerous places that are difficult to access [2]. Even in the most optimistic predictions, oil prices will rise over the coming years as oil production steadily declines [3].

The consequences of peak oil go beyond energy crisis. International trade is driven by oil. Without cheap methods of transporting goods, global capitalism will suffer.

International relations will also suffer, as oil wars are already happening and will only get worse. As oil prices climb and recession worsens, public health will also decline [4]. Agriculture, which is highly dependant on fossil fuels, will also suffer greatly [2].

Fossil fuels including oil currently provide for over 85% of energy needs in the United States [5]. The International Energy Agency and the U.S. Department of Energy predict that world oil demand will climb from 85 million barrels per day presently to 120 million barrels per day by 2030 [2]. To counter the effects of decreased oil availability, new sources of energy need to be developed along with more efficient uses of energy.

One new source of energy is a compost pile. The energy from a hot compost pile can be used to charge batteries with thermoelectric modules. Work has already been done to charge batteries with thermoelectric modules using waste energy sources. However, no one outside of Ithaca College has yet considered using a compost pile to charge batteries with thermoelectric modules. This idea is innovative and also doubly sustainable because it takes something that is already repurposing waste (compost) and getting even more out of it than expected. This project is a new and innovative use of the already existing, but not widely used, technology of thermoelectric modules coupled with the age old and already sustainable technology of compost.

1.2 Previous Work

In the summer of 2007, Colin Howard started work on a Compost Thermal Heating Project. Howard's goal was to reduce Ithaca College's carbon footprint by analyzing the potential of generating electricity from compost piles. He mapped the thermal profile of a compost pile at the Cayuga Compost Facility by recording the temperature of different sections of the pile, and found that the hottest part of a pile is in the middle

at about 60 °C. Next, he used this information to create a laboratory replication of the temperature difference between the compost pile and a cold winter day, about 60 °C. He used two 2.5 W Hi-Z thermoelectric modules connected in series to turn this temperature difference into a voltage difference that could charge a battery. The apparatus he used is the same one that I continued to use, which is described in detail in the methodology section. By connecting a 12 Volt DC-DC converter to the modules to increase the voltage at the cost of current, he was able to fully charge a 12 Volt battery [6]. This project is a continuation of Howard's research.

Other researchers have developed thermoelectric battery chargers. Yu and Chau took advantage of the waste energy generated by internal combustion engine automobiles. They used a Maximum Power Point Tracking (MPPT) technique to maximize the power output that was used to charge the battery. Since fuel combustion wastes about 40% of the energy input, the exhaust manifold heats up to 250 °C. The changing voltage across the battery was tracked during charging, instead of across the thermoelectric terminals, which is usually done for MPPT. This new method took into account the non-constant power loss from the Cuk DC-DC converter that was used for power conditioning. Six thermoelectric modules were connected in series in a setup similar to Howard's, except that the heat sink and thermal spreader were copper, not aluminum. Voltage, current, and power were measured for different loads, and were used to find the internal resistance of the module system, which varied with temperature. Since the maximum power is obtained from the system at matched load, the load impedance must be controlled as the temperature changes. The input impedance of the DC-DC converter is a function of its duty cycle, so the power to the battery can ultimately be controlled by varying the duty cycle. A perturb-and-observe technique was used by a computer to control the duty cycle, by continually perturbing the duty cycle slightly, observing if the power increased or decreased, and

adjusting accordingly until the maximum power was reached. This method showed power improvements of up to 14.5% and 22.6% compared with methods using no MPPT and no power conditioning, respectively [7].

Qiu and Hayden used a thermoelectric generator to create a self-powered heating system. The generator, which produced 550 W, used energy from a fuel-fired furnace to cover all of its electrical needs. In this way, the system was deemed to be 100% efficient because all of the energy produced by the heater was used, either to power itself or to warm the house [8].

Rahman and Shuttleworth developed a thermoelectric battery charger to charge a laptop computer battery. The goal was to design a portable source of energy that would extend the life of the battery, since the need to charge the laptop's battery limits its portability. The system used butane gas from a camping cooker as an energy source. A boost DC-DC converter was used to match the 12-Volt input of the laptop. The setup of their thermoelectric converter system was similar to Howard's. A major difference was the energy source, which was butane. The module used was also a higher power Hi-Z module. The temperature difference was much higher than Howard had, with the hot side being at a constant 250 °C and the ambient temperature was 20 °C. A fan was used to draw energy away from the cold side. A blocking oscillator was used to provide the power necessary to activate the converter until the module output was high enough. The output of their system was 5 Watts, which doubled the life of their laptop computer's battery [9].

Eakburanawat and Boonyaroonate developed a thermoelectric battery charger that, like Yu and Chau's, also used MPPT. Their system used a single-ended primary inductance converter (SEPIC) DC-DC converter controlled by a microcontroller. Six 5.9 Watt TE modules from Taihuaxing Co. Ltd were used in series. Like Yu and Chau's setup, the microcontroller controlled the duty cycle of the DC-DC converter

to obtain maximum output power from the modules. The efficiency of the DC-DC converter was found to be 95.11% when using MPPT. The maximum charging power of the system was found to be 7.99 W, which was better than direct charging by 15% [10].

It has been found that thermoelectric modules can be used to charge batteries. It has also been found that thermoelectric modules work well with waste energy. Since compost generates waste energy, we should be able to use compost energy to charge batteries with thermoelectric modules.

1.3 Goals

Howard's thesis proved the concept that a battery can be charged using thermoelectric modules at the temperature difference between the center of a compost pile and cold ambient air. My goal was to find the most efficient way to do this.

Since the hottest part of the compost pile is the center, that energy needs to be brought to the outside where the thermoelectric modules would be. I sought to find the most effective way of bringing the most amount of energy from the middle of the pile to the outside.

The maximum amount of power produced by the modules is necessary to know. Specifically, I wanted to find out exactly how much power one thermoelectric module could produce when held between a temperature difference of 60 °C. I am specifically focusing on this temperature difference because it is taken to be the ideal temperature difference between the hot compost pile and a cold winter day. Since a device's maximum power is produced at matched load [11], I also needed to find the internal resistance of the module. More importantly, I needed to find out if the internal resistance changed if the temperature difference changed, since neither compost nor

ambient air stay at a constant temperature.

All this information can be used in future continuations of this project to design an efficient apparatus that takes waste energy from the compost, brings it to the modules, and charges household batteries in an efficient way.

Chapter 2

Theory

2.1 A Compost Pile

In order to understand where a compost pile's waste energy comes from, the inside of the pile needs to be explored. The generation of heat energy is a byproduct of the breakdown of organic material, mostly by bacteria. Two types of bacteria can present in compost depending on what stage of breakdown the pile is in, mesophilic or thermophilic bacteria. Mesophilic bacteria thrive at temperatures between 15 °C and 40 °C. Thermophilic bacteria thrive at temperatures between 45 °C and 80 °C. Other microorganisms that live in compost include protozoa, rotifers, fungi, and actinomycetes. A compost pile is also home to many invertebrates that feed on microbes and other invertebrates, including worms, centipedes, beetles, and spiders [12].

A pile has three stages: mesophilic (moderate temperature), thermophilic (high temperature), and the cooling and maturation phase. During the mesophilic stage, the temperature gradually increases as mesophilic microbes inside the pile break down the organic material. In an industrial-sized pile this phase lasts three to five days.



Figure 2.1 Industrial compost piles are long windrows several feet wide and tall [13].

The thermophilic phase is the most important phase when considering compost as an energy source. During this stage, temperatures reach 60 °C to 70 °C. Thermophilic microbes decompose the material rapidly at this hot stage, during which pathogens, fly larvae, and weed seeds are destroyed. The Environmental Protection Agency (EPA) regulates that compost must be kept above 40 °C for at least five days, and above 55 °C for at least four hours in order to kill any pathogens that are living in the compost. These regulations keep the pile at high temperatures for an extended period of time, providing the steady energy output needed to charge a battery. The pile must be turned for aeration regularly, which results in new temperature peaks. Turning exposes new material and replenishes oxygen [12]. Turning usually occurs on a weekly basis [6], so a charger could be left in the pile for an extended period of time. After the thermophilic stage, mesophilic microbes once again take over for the cooling and maturation phase. In this stage, chemical reactions continue within the pile as the compost lowers to nearly ambient temperature. This phase makes the compost stable and better for plant use [12].

A compost pile's energy is lost in many ways. Through conduction, energy is transferred within the compost to the air molecules outside, resulting in energy loss. Hot air rising within the pile causes energy loss through convection. Energy from the warm pile also radiates out into the cooler air. Sometimes steam can be seen rising from a pile. In this case energy is also being lost through the latent heat of evaporation as water in the pile is turned into steam [12]. All of this energy that is going to waste can be taken advantage of to charge a battery.

An industrial-sized compost pile is shown in Fig. 2.1. The center is the hottest part of the pile at 60 °C, with the edges at cooler temperatures [6]. In order to take the most advantage of compost energy, the energy in the center needs to be brought to the outside, where a device can use this energy to charge batteries. The center

may be several feet away from the outside edge, so a metal rod or other device will need to be placed in the pile to serve as a mechanism of energy transfer. If T_{CH} is the temperature of the inside of the compost and T_{CC} is the temperature of the outside end of the energy-carrying metal rod, then the percentage of the compost energy that can possibly be used for charging batteries is

$$\text{Percent} = \frac{T_{CH} - T_{CC}}{T_{CH}}. \quad (2.1)$$

It is desirable for this percentage to be as high as possible in order to use the compost energy most efficiently. In order to optimize this, different energy transfer mechanisms must be explored.

2.2 Batteries

A battery consists of one or more cells, which are made up of the three main parts seen in Fig. 2.2: the anode, the cathode, and the electrolyte. Using these parts, a cell goes through a redox reaction to convert chemical energy into electrical energy [14]. When a load is attached to the terminals of a cell, the anode is oxidized, meaning it gives up electrons to the circuit, while the cathode is reduced, meaning it accepts electrons from the circuit. The electrolyte is an ionic conductor through which anions and cations can travel between the electrodes. When the load is attached, electrons travel from the anode, through the load, and back to the cathode, creating an electrical current. To charge a rechargeable battery, a DC power supply is connected to the terminals of the battery instead of a load, and the flow is reversed, charging the battery.

There are two basic types of batteries: primary batteries and secondary batteries. Primary batteries are not rechargeable. In general these batteries are called “dry

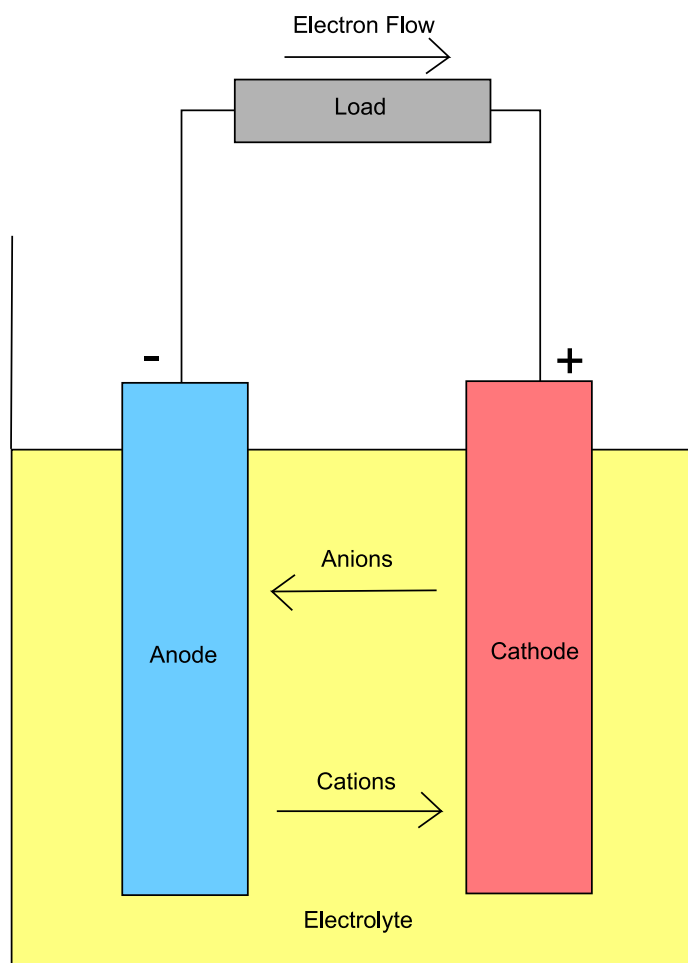


Figure 2.2 Batteries convert chemical energy into electrical energy through a redox reaction. When a load is connected to the terminals, electrons flow from the anode, through the load, and back to the cathode, creating an electrical current.

cells” because the electrolyte is held in an absorbent material, so there is no liquid electrolyte. Secondary batteries are capable of being recharged. These are useful for energy storage in machines like cars, where they are charged by the machine as it is running so they can deliver energy when needed. These batteries can also be used just like a primary battery, except they are recharged instead of thrown away. In this project, only secondary batteries are dealt with.

Secondary batteries have high power densities, high discharge rates, flat discharge curves, and good low temperature performance. It is important to note the depth of discharge of a battery, which is the fraction of power that can be withdrawn from the battery. After discharging a battery below a certain voltage, it is permanently damaged.

The time rate of charge is determined by how much current is allowed into the battery by the charger. Some batteries can handle higher voltages for shorter amounts of time without overheating, while some need lesser voltage and more time. “Smart” chargers have built-in voltage regulators to dissipate the charging current once the battery’s maximum voltage is reached. Ideally, the charger built to work from compost should be a smart charger that shuts off when the battery is fully charged.

For the charger in this project, rechargeable Nickel-Metal Hydride (NiMH) were explored, because this type of battery is widely used. NiMH batteries are charged using a constant current of 10% to 100% of the battery’s capacity, depending on how fast the battery needs to be charged. To avoid overcharging, faster battery chargers lower the current to a “topping” charge of 10% capacity after a certain amount of time, or when the charger detects a certain voltage, temperature, or temperature differential in the battery. The charging curves for Ni-MH following these three factors can be seen in Fig. 2.3.

On the voltage curve it can be seen that when the battery is fully charged, the

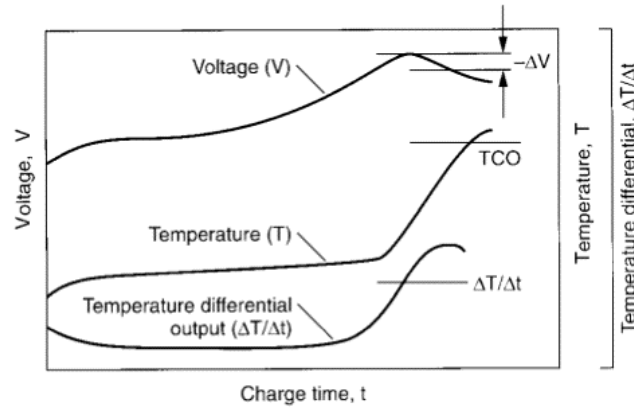


Figure 2.3 Charging curves for a NiMH battery [14]. The curves follow the voltage, temperature, and temperature differential of the battery as it charges. A “smart” battery charger will track one or more of these factors and stop charging once a certain level is reached.

voltage drops. If the battery charger is tracking voltage, it stops charging once that voltage drop is detected. If the charger is monitoring temperature, charging is stopped once the battery reaches a temperature that signals overcharging. If the charger tracks temperature differential, it will monitor the rate of temperature increase and terminate charging once a predetermined rate has been reached [14].

2.3 Thermoelectric Modules

The Seebeck effect describes the voltage produced when the junction between two dissimilar metals (a thermocouple) are held at two different temperatures, called the Seebeck or thermoelectric voltage:

$$V_S = \alpha_{ab} (T_H - T_C), \quad (2.2)$$

where α_{ab} is the Seebeck coefficient of the junction between the two materials, and is

given by

$$\alpha_{ab} = \alpha_a - \alpha_b. \quad (2.3)$$

The Seebeck coefficient is the property of a material that determines the magnitude of the thermoelectric voltage created when a temperature difference is applied across the material. The thermoelectric voltage results from the dissipation of charge carriers from the hot side, where the carriers have greater kinetic energy, to the cold side of the material, building up charge. Thermoelectric materials that work the best have high Seebeck coefficients, high electrical conductivities, and low thermoelectric conductivities. A high electrical conductivity results in better transfer of charge carriers, and a low thermal conductivity ensures that little energy is transferred due to heating, keeping the two ends at the greatest temperature difference possible. The figure of merit, Z , of a material describes how well the material will work thermoelectrically:

$$Z = \frac{\alpha^2 \sigma}{\lambda}, \quad (2.4)$$

where σ is electrical conductivity and λ is thermal conductivity [15].

The thermoelectric module used in this project, shown in Fig. 2.4, consists of 97 thermocouples attached electrically in series and thermally in parallel (side by side). The modules I used are made of bismuth telluride based semiconductors. The couples consist of N-type and P-type semiconductors. N-type semiconductors have an abundance of free electrons (carriers), which is obtained by doping. In the doping process for an N-type semiconductor, a five valence material is introduced into the crystal lattice of a four valence material. This results in unbounded electrons, which can be easily excited into the conduction band, creating electric current. P-type semiconductors have an abundance of “holes,” which is obtained by a different kind of doping where a trivalent material is introduced into a four valence crystal lattice.

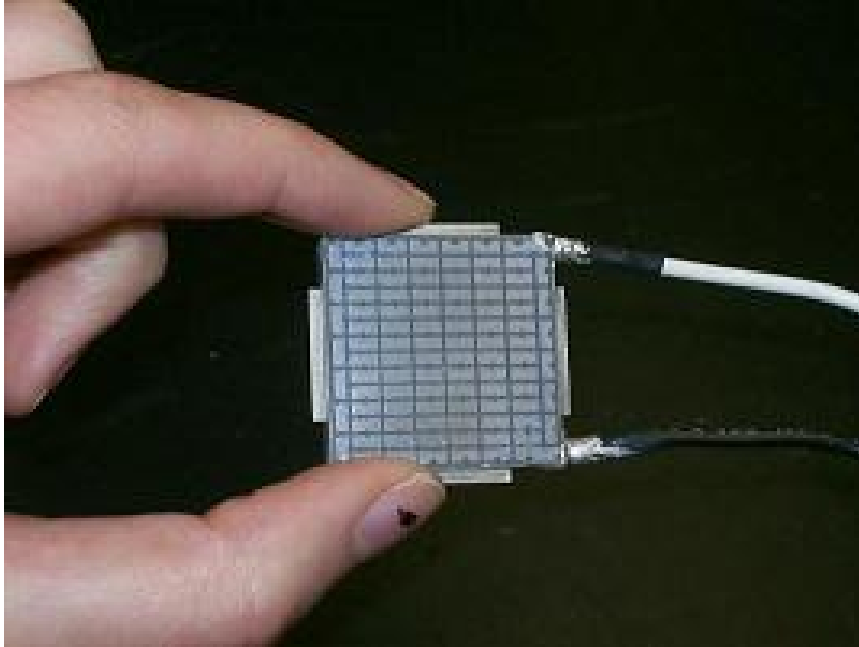


Figure 2.4 The Hi-Z 2.5 W thermoelectric module that was used for this project.

As electrons fill the “holes,” electric current is produced. The holes and free electrons in the semiconductors are called charge carriers. As seen in Fig. 2.5, these charge carriers move from the hot end of a thermocouple to the cold end, creating a voltage and, if a load is attached, a current.

One thermocouple produces a low voltage and a high current [15]. So, in order get a larger voltage, many thermocouples need to be attached electrically in series and thermally in parallel, forming a module.

When using a thermocouple made of N-type and P-type semiconductors, the voltage V created across the terminals when a temperature difference ΔT is applied is

$$V = \alpha_{pn}\Delta T, \quad (2.5)$$

where α_{pn} is the difference between the Seebeck coefficients of the two semiconductors. When a load R_L is attached to the terminals, the current that flows across the load,

according to Ohm's Law, is

$$I = \frac{\alpha_{pn}\Delta T}{R + R_L}, \quad (2.6)$$

where R is the internal resistance of the thermocouple. From Eq. 2.5 and Eq. 2.6 the power output of a thermocouple can be found:

$$P = VI = \frac{(\alpha_{pn}\Delta T)^2}{R + R_L}. \quad (2.7)$$

The power output of a thermocouple, and consequently of the module, should be proportional to the square of the temperature difference.

The modules used were made by Hi-Z Technology, Inc, which provides a manual that describes ways to obtain the most power output from the module. Good thermal contact between the module and the energy source is required, and applying pressure helps increase thermal contact [17]. It is also recommended that a thin slab of aluminum or copper be used between the module and the energy source as a thermal spreader for an even distribution of energy. A thermal transfer compound such as thermal grease should be used to fill in surface irregularities that might decrease thermal contact. An electrically insulating material such as a ceramic wafer should be placed between the module and any metal surface to avoid short circuiting. The Hi-Z website also provides a table of the properties of the H-2 module used in this project, shown in Table 1.

As seen in Table 1, the efficiency of the module is quite low. This means that the module needs a large temperature difference in order to get a non-negligible current out of it. At first the low efficiency makes it seem like the module is not using energy wisely. However, given that this project's aim is to utilize waste energy, harnessing

Table 1. Properties of the 2.5 Watt H-2 model thermoelectric module used in this project [18]. * At design temperatures ** At matched load

Physical, Thermal, and Electrical Properties	Value	Tolerance
Width & Length	2.90 cm	± 0.25 cm
Thickness	0.508 cm	± 0.25 cm
Weight	13.5 g	± 2 g
Compressive Yield Stress	20 MPa	minimum
Number of Active Couples	97	—
Design Hot Side Temperature	230 °C	± 10 °C
Design Cold Side Temperature	30 °C	± 5 °C
Maximum Continuous Temperature	250 °C	—
Maximum Intermittent Temperature	400 °C	—
Thermal Conductivity*	0.024 W/cm*K	+0.001
Heat Flux*	9.54 W/cm ²	± 0.5
Power**	2.5 Watts	minimum
Load Voltage	3.3 Volts	± 0.1
Internal Resistance	4.0 Amps	± 0.05
Current	0.8 Amps	± 1
Open Circuit Voltage	6.53 Volts	± 0.3
Efficiency	4.5%	minimum

any small amount of energy that will go to waste is an accomplishment. So, the low efficiency of the module is currently not a concern.

2.4 Maximum Power Point Tracking

The power output of a module P when a load R_L is attached can be calculated from the measured voltage across the leads V_L and the current through the load I_L :

$$P = V_L I_L = \frac{V_L^2}{R_L} \quad (2.8)$$

When the load is varied, the power output is also varied, as seen in Eq. 2.8. The maximum power output of any device occurs at matched load [11], or when the load resistance R_L is equal to the device's internal resistance R_{int} . If the internal resistance of the device fluctuates for any reason, that resistance needs to be tracked if the maximum power output is desired at all times. A maximum power point tracking (MPPT) device tracks these fluctuations in order to produce consistent maximum power. Solar panels already make use of this technology for varying amounts of sunlight. In the case of thermoelectric modules, the internal resistance may vary with varying temperature. A compost pile will not have a perfectly constant temperature, nor will the ambient air, so an efficient compost-powered battery charger will make use of maximum power point tracking. It is important to obtain the most amount of power possible because power is energy per time. A high power output will charge batteries in less time, making for a more attractive product.

The internal resistance of the module can be found using measurable values [10]:

$$R_{int} = \frac{V_{OC}}{I_L} - R_L, \quad (2.9)$$

where V_{OC} is the open-circuit voltage across the module leads. This can be tested

for various temperature differences to find out how the internal resistance varies with temperature.

Chapter 3

Transferring Energy from Compost to Module

3.1 Methodology

The hottest part of a compost pile is in the center, which may be several feet away from the outer edge of a large pile. My first concern was to figure out how to bring this energy from the center to the outside, where it can be used. I determined that a good way of doing this would be to use a metal stake or rod that would carry energy from the center to the outside. The stake would need to be insulated from the cooler compost near the edges so that as much energy could be transferred as possible.

Slabs of copper and aluminum of similar lengths were tested to see which would carry energy the most efficiently. Since copper has a higher thermal conductivity than aluminum, copper was expected to transfer the most energy. Rags wrapped around each slab provided a small amount of insulation during the experiment, shown in Fig. 3.1. A few inches were left bare at either end of the slab. One end was placed on a hot plate and the other was rested on the heat sink. Weights were placed on

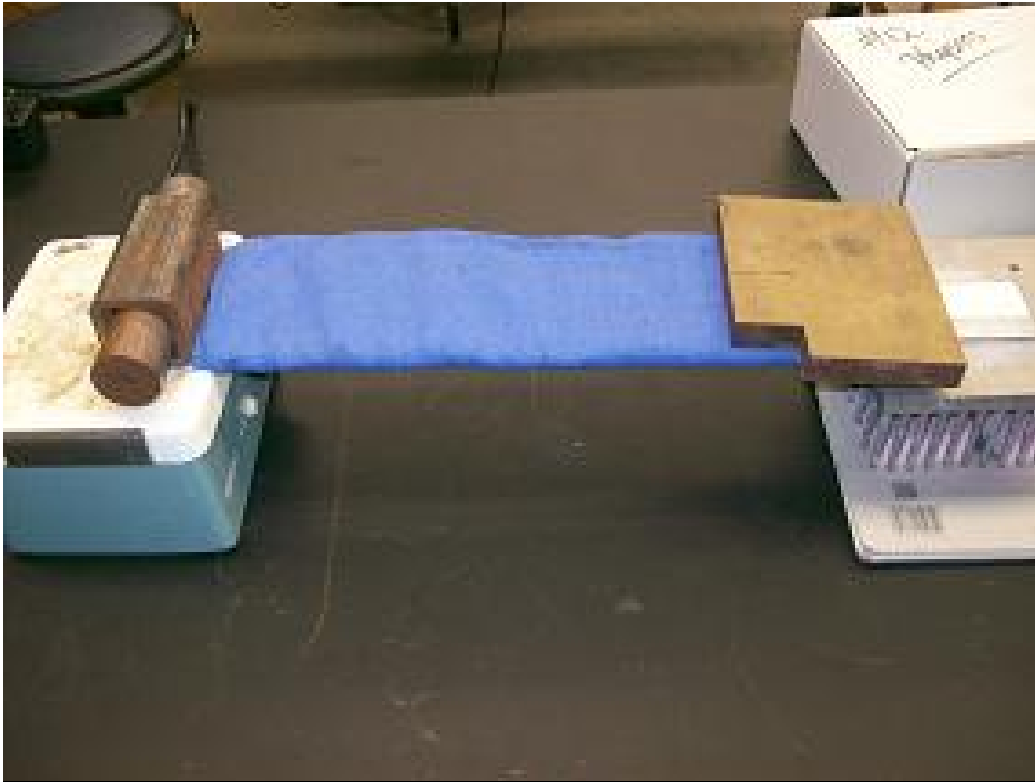


Figure 3.1 To test for thermal conductivity of the metal, a slab of metal was insulated with rags. One end was rested on a hot plate and the other on a heat sink. As one end was heated, the temperatures of both ends were monitored to see how much energy transferred from the hot end to the cold end. Weights were used on each end to increase thermal contact with the surface.

each end to increase thermal contact, as shown in Fig. 3.1. Thermistor sensors were taped to the top of each end of the slab, and the temperature difference between the two ends was recorded using Data Studio software on a PC.

Once one metal was determined to transfer the most energy, different types of insulation were tested. The apparatus was set up in the same way, shown in Fig. 3.2, with the metal slab resting on the hot plate and the heat sink. Insulations tested were fiberglass batting with an R-value of 3.14 - 4.30 per inch, pipe insulation with an R-value

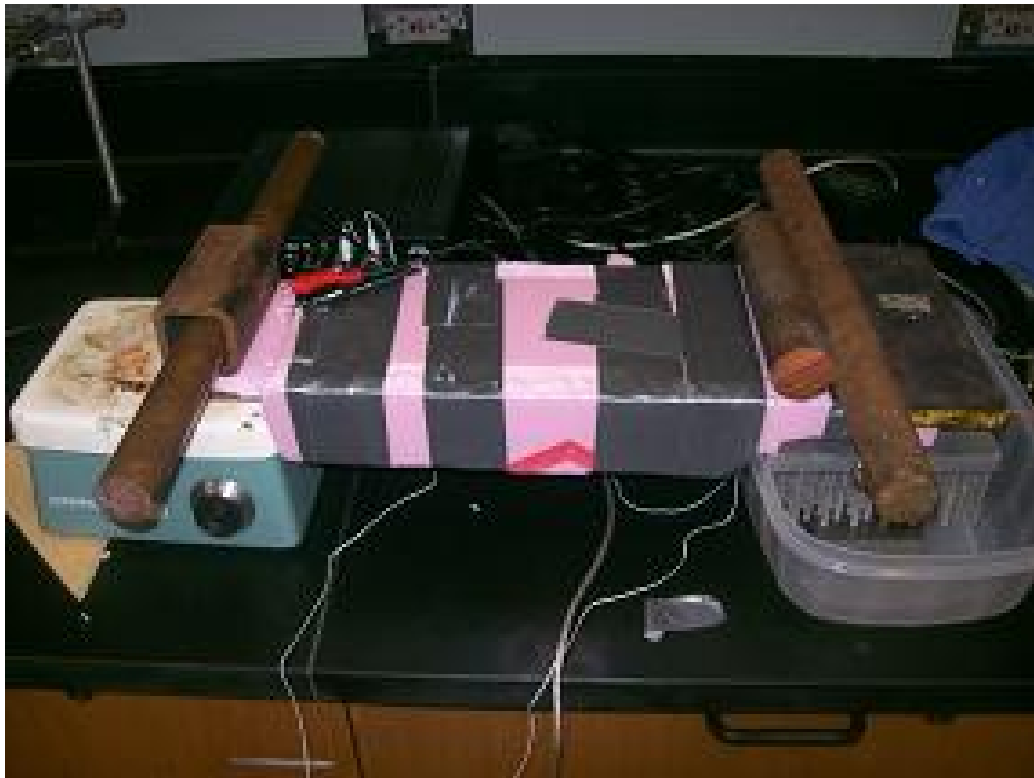


Figure 3.2 To test insulations, the setup remained the same while the metal was insulated with various insulations. Here, extruded polystyrene is shown.

of 3.3 per inch that was foiled on one side, and one inch thick extruded polystyrene with an R-value of 5.00 per inch. Based on R-values, the extruded polystyrene was expected to work the best.

3.2 Data and Analysis

Copper and aluminum were tested for thermal conductivity by heating one end of a metal slab lightly insulated with rags and monitoring both ends. Copper was found to transfer more energy than aluminum when only insulated with rags, as shown in Table 2. Copper was then tested with different insulations in place of the rags. Extruded polystyrene was found to insulate the best, as shown in Table 2, allowing $86\% \pm 2\%$ of energy to travel from one end of the copper slab to the other. The percentage of energy transferred was found using Eq. 2.1, with T_{CH} being the temperature of the hot side of the metal slab and T_{CC} being the temperature of the cold side. The temperature difference ΔT_C was found by subtracting the hot side temperature from the cold side temperature. The amount of energy transferred using various metals and insulations is shown in Table 2.

It can be seen that the foiled pipe insulation did not work any better than rags as insulating material. This is concerning, given that the pipe insulation had a fairly high R-value. The pipe insulation's lack of performance was probably due to the way it was wrapped around the copper slab. It was difficult to keep from compressing the insulation around the corners of the slab, which decreased the amount of dead air between the fibers and therefore decreased its insulating capabilities. The extruded polystyrene, on the other hand, was stiff so it was not possible to compress it. Even though the extruded polystyrene worked the best, it still only allowed for $86\% \pm 2\%$ of the energy to be transferred, which is a significant energy loss.

Table 2. Transfer of energy using various materials

Material and Insulation	ΔT_C	Energy Transfer Percentage
Aluminum with Rags	$16^\circ\text{C} \pm 1^\circ\text{C}$	$65\% \pm 3\%$
Copper with Rags	$18^\circ\text{C} \pm 1^\circ\text{C}$	$71\% \pm 2\%$
Copper with Fiberglass Batting	$16^\circ\text{C} \pm 1^\circ\text{C}$	$75\% \pm 2\%$
Copper with Foiled Pipe Insulation	$18^\circ\text{C} \pm 1^\circ\text{C}$	$71\% \pm 2\%$
Copper with Extruded Polystyrene	$9^\circ\text{C} \pm 1^\circ\text{C}$	$86\% \pm 2\%$

Error was found using the following equation, derived from the general error propagation formula [19] and Eq. 2.1.

$$\delta\text{Percent} = \sqrt{\left(\frac{100T_{CC}}{T_{CH}^2}\right)^2 + \left(\frac{100}{T_{CH}}\right)^2} \quad (3.1)$$

The error in raw temperature measurement was $\pm 1^\circ\text{C}$.

3.3 Discussion

The best combination of metal and insulator, copper with extruded polystyrene, transferred $86\% \pm 2\%$ of energy from one end to the other. Maximum energy transfer efficiency is crucial because the power output of the thermoelectric module is temperature dependent. Energy transfer could be maximized by using a thicker slab of material. The copper slab used was fairly thin, about a half an inch thick. Thermal

conductivity improves with a greater cross-sectional area, so a thicker slab would be preferable.

Considerations also need to be made that the surrounding compost could damage any device that is placed in it. The energy transfer device would need to be protected from the compost, possibly with PVC piping or another protective material that would not break down in the compost. Such a material would have its own insulating qualities that might increase the percent of energy transferred. This will need to be taken into account in future developments of the project.

Chapter 4

Efficient Use of Modules

4.1 Methodology

Compost conditions were replicated in the laboratory. A hot plate was used as the energy source, replicating hot compost, and ice water was used to replicate cold ambient air. One thermoelectric module was placed between a small slab of aluminum and an aluminum heat sink. The aluminum slab served as a thermal spreader to insure even distribution of energy over the module, while the heat sink drew energy away from the cold side of the module. The module was insulated from the surrounding metal by ceramic wafers, which are thermally conducting and electrically insulating. Thermal grease was used to stick the wafers to the spreader and the sink. Thermal grease was also used between the module and the wafers to seep into the small crevices on the surface of the module, ensuring the greatest thermal contact. Thermistors were attached to the sink and the spreader as close to the module as possible to monitor the temperature of the hot and cold sides of the module. In order to keep everything together, and to again increase thermal contact through pressure, the spreader was bolted to the heat sink. The space between the spreader and the heat sink was

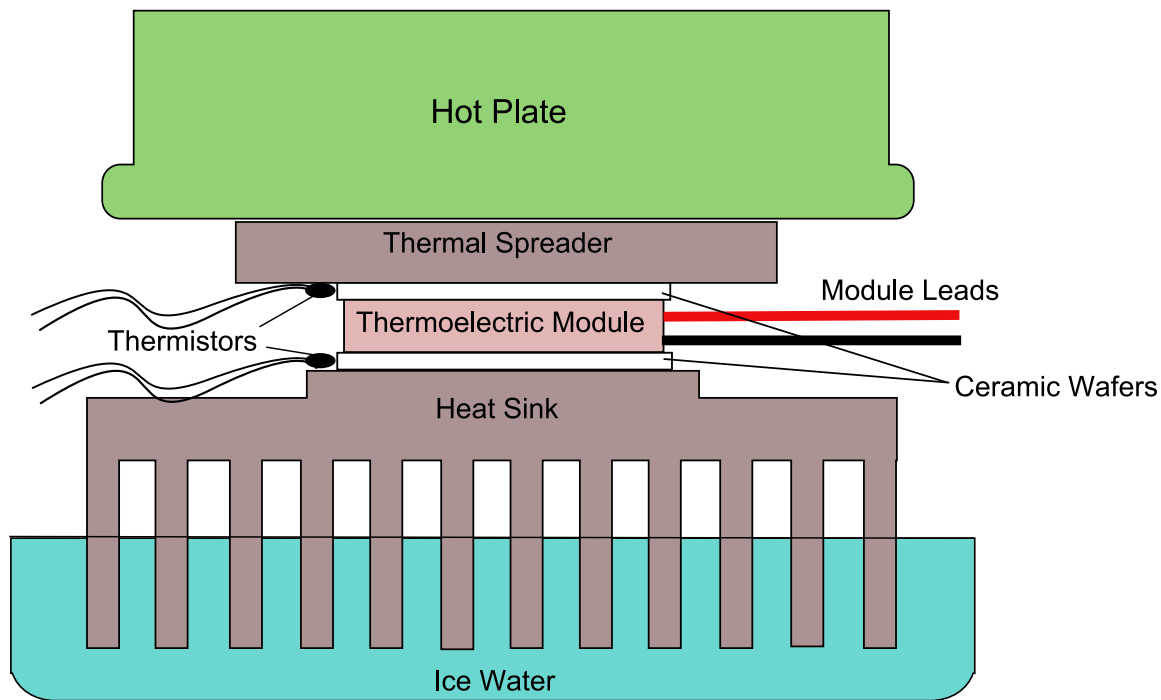


Figure 4.1 A module is placed between a hot plate and a heat sink in ice water. The hot plate replicates a hot compost pile while the ice water replicates cold ambient air. The thermal spreader ensures that energy from the hot plate is distributed evenly over the surface of the module. The heat sink draws energy away from the cold side of the module. The ceramic wafers electrically insulate the module from the surrounding metal.

measured and compared on each side to make sure that the spreader was pressing evenly on all corners of the module. Adjustments were made as necessary to ensure that the space between the spreader and the sink was the same on all sides.

The whole apparatus was placed with the fins of the heat sink in ice water. A hot plate was placed upside-down on the aluminum spreader. Once the hot plate was turned on, the ice water was stirred occasionally to force convection and ensure that energy was being drawn away from the cold side of the module at a sufficient rate. This procedure was followed for all parts of the following experiment.

First I wanted to find out how much power could be produced from one module at a variety of temperature differences. The module leads were connected to a decade box which served as the variable load in Fig 4.2. The current and voltage were measured throughout the experiment using a PASCO current sensor and a PASCO voltage sensor, respectively. The temperature difference across the module was kept constant by adjusting the knob on the hot plate and stirring the ice water as needed. The decade box was set at a high resistance, $500\ \Omega$, to begin, to create a very large load. Once a constant temperature was reached, the resistance was lowered. Every 100-200 seconds, the resistance was lowered again, until the resistance reached zero. A point was taken by Data Studio every second, providing a large amount of data for each resistance and thus ensuring consistency. Data Studio was used to plot temperatures of the hot and cold sides of the modules and the difference between them in real time so that temperature adjustments could be made as necessary. On a separate computer, Data Studio recorded voltage and current as the experiment ran. A graph was plotted as data was taken of voltage against current, also in real time. Another graph was plotted as data was taken of power against current. Power was calculated by Data Studio from current multiplied by voltage. This procedure was followed for temperature differences of $10\ ^\circ\text{C}$ to $70\ ^\circ\text{C}$ in $10\ ^\circ\text{C}$ intervals.

The first module behaved strangely, as described in the data section, and was abandoned after a few runs. A second module was used and produced more consistent results. Finally, a new module was ordered to test, to see if the results of the brand new module agreed with the results of the second module. The circuit setup changed slightly for the third module to obtain more direct results. In the first circuit shown in Fig 4.2, the voltage was taken across the variable resistor, not including the ammeter. This meant that the power results and internal resistance results were for both the module and the ammeter in series. Since the ammeter has an internal resistance of

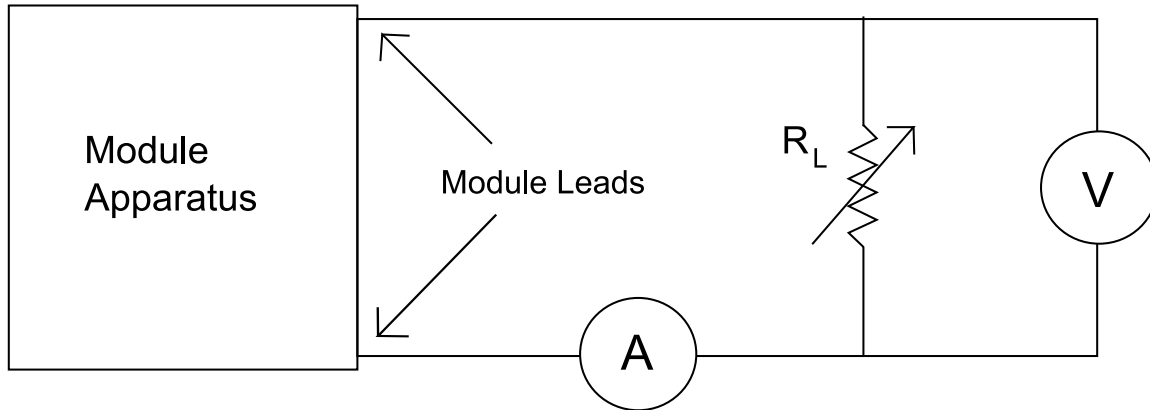


Figure 4.2 The module apparatus is connected to a variable load. The voltage and current are monitored to observe how the power output changes with the varying load.

1.00 Ω , this meant that the power that was calculated directly was not accurate for the module by itself. When finding the internal resistance of the second module, the ammeter's resistance needed to be subtracted from the result in order to obtain the module's resistance. The new circuit in Fig.4.3 was set up and the procedure above was followed again for the third module for the same temperature differences. In this circuit, the voltage was measured across the module leads, so all results were for the module itself, not including the ammeter.

4.2 Data

4.2.1 First Module

The current and voltage were recorded against time for the first module as the resistance was varied from 500 Ω to zero. Temperature differences of $10^\circ\text{C} \pm 1^\circ\text{C}$, $20^\circ\text{C} \pm 1^\circ\text{C}$, and $30^\circ\text{C} \pm 1^\circ\text{C}$ were tested. While the experiment was running, the voltage and current dropped at random times. This behavior worsened with higher

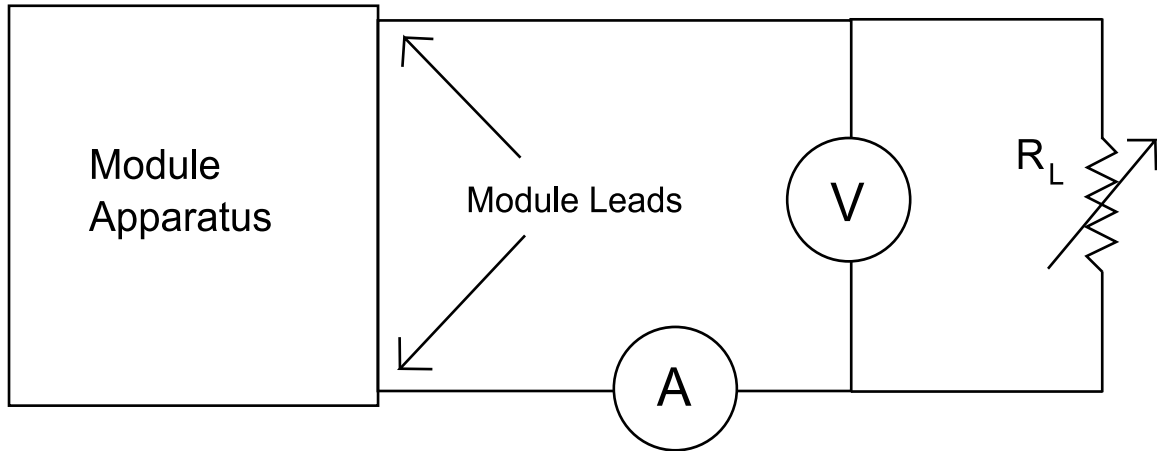


Figure 4.3 The setup was changed so that the voltage is monitored across the module leads instead of the load. This was because the ammeter has an internal voltage that must be taken into account.

temperatures, and by 30°C it was very sporadic, as seen in Fig. 4.4. As resistance is decreased, the current should steadily increase while the voltage steadily decreases, according to Ohm's Law:

$$I = \frac{V}{R}. \quad (4.1)$$

I found no explanation for these random drop-offs other than malfunction of the module. The malfunction was likely caused by bad connectivity of the module leads, which were fraying. I attempted to repair the junction of the leads to the module with cold solder, but the strange behavior continued. The V-I curve along with the power curve of the module were plotted by Data Studio as the experiment ran. These graphs are shown in Fig. 4.5. These plots look very messy compared to the same plots from the second and third modules. The power output of the first module is also significantly lower than the second and third modules for the same temperature difference, further suggesting a damaged module.

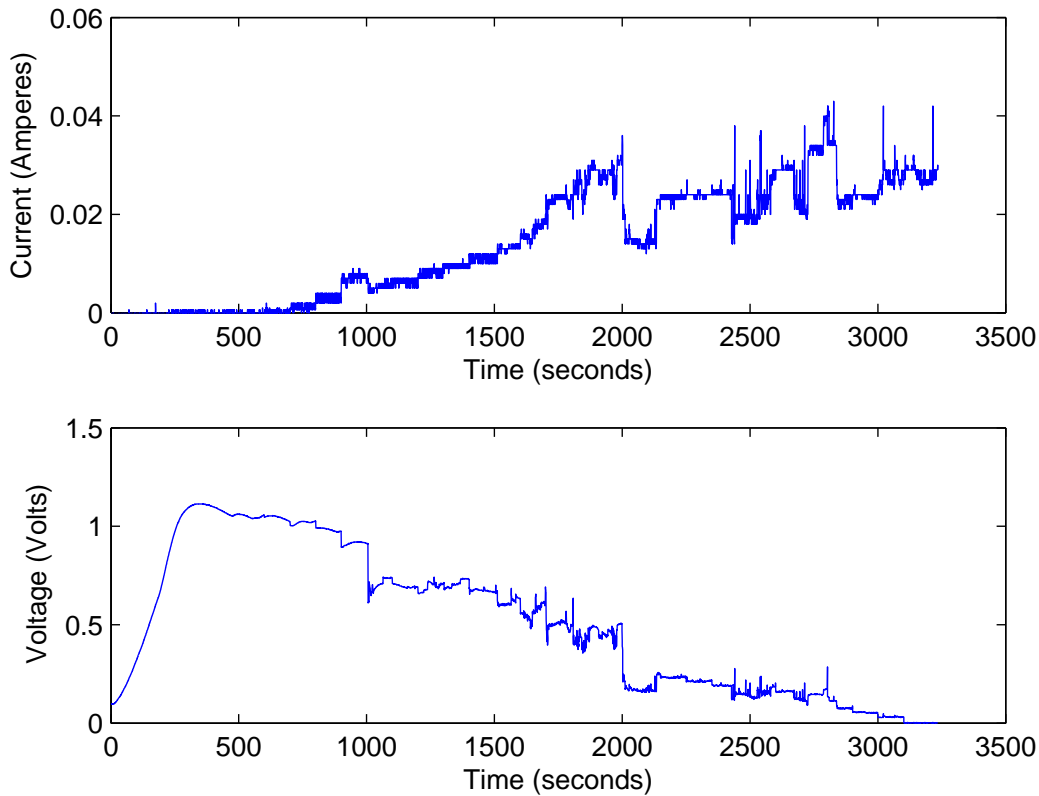


Figure 4.4 The voltage and current against time of the first module tested for a temperature difference of $30^{\circ}\text{C} \pm 1^{\circ}\text{C}$. The voltage and current dropped for no reason at random points, which indicated damage in the module. The error in current and voltage measurements were $\pm 0.005\text{ A}$ and $\pm 0.005\text{ V}$, respectively.

4.2.2 Second Module

When the second module was tested there were no current or voltage drop-offs, as seen in Fig. 4.6 - 4.7 for a $60^{\circ}\text{C} \pm 1^{\circ}\text{C}$ temperature difference, which is the ideal difference between a hot compost pile and a cold winter day. I questioned the accuracy of these results, because the lead junctions on the second module were also becoming loose and starting to fray, although the damage was not yet as great as on the first module. The voltage steadily falls and the current steadily rises as the resistance is

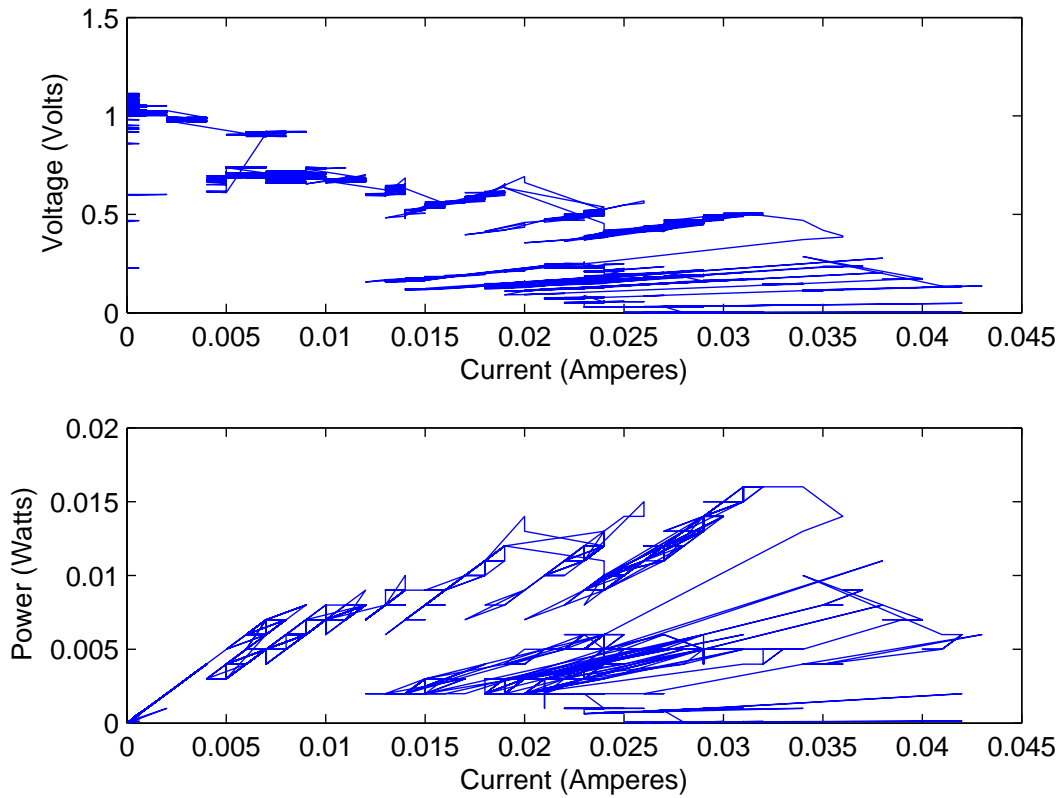


Figure 4.5 The power curves of the first module tested for a temperature difference of $30^{\circ}\text{C} \pm 1^{\circ}\text{C}$. The curve is very erratic, again indicating damage in the module.

decreased, as expected. The staircase appearance is caused by the discrete changes in resistance, since the resistance could not be decreased by less than $1\ \Omega$ at a time. The V-I curve, which describes how the module will behave in a circuit and is seen in Fig. 4.7 is linear. Not all devices have a linear V-I curve. Batteries do, but solar panels do not. The power curve follows a parabolic curve, peaking in the middle at $394\ \text{mW} \pm 7\ \text{mW}$ for a $60^{\circ}\text{C} \pm 1^{\circ}\text{C}$ temperature difference.

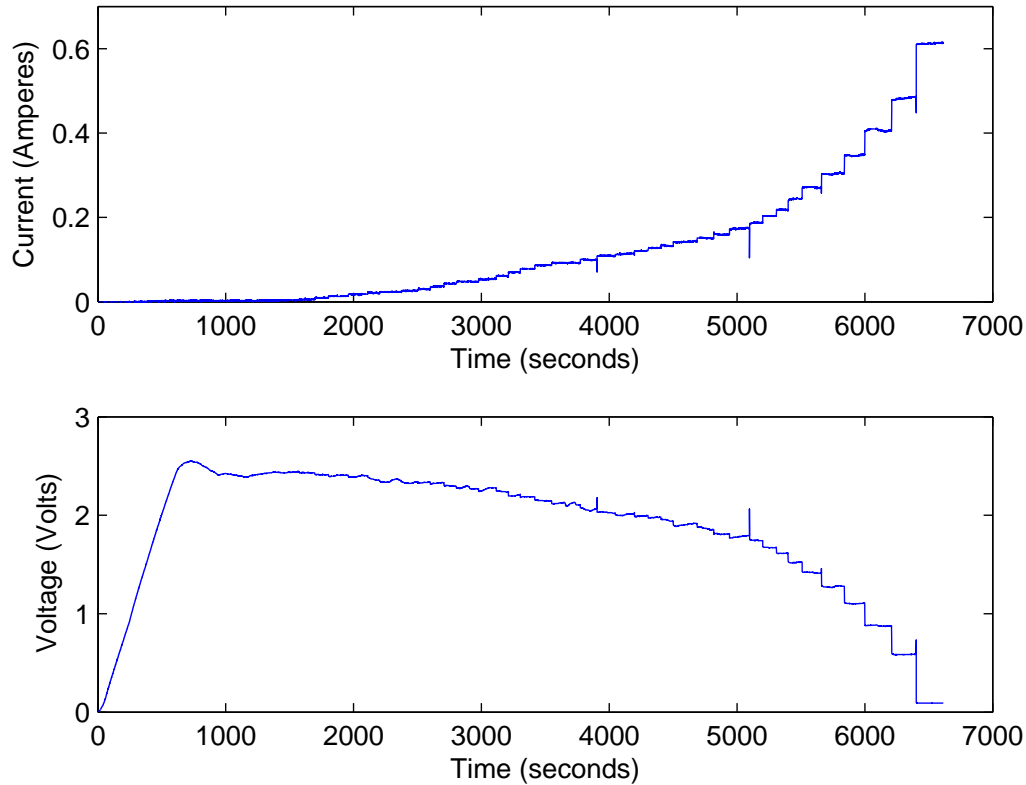


Figure 4.6 The voltage and current against time of the second module tested at a $60^{\circ}\text{C} \pm 1^{\circ}\text{C}$ temperature difference. As the resistance is lowered over time, the current increases and the voltage decreases, as expected. The error in current and voltage measurements were $\pm 0.005\text{ A}$ and $\pm 0.005\text{ V}$, respectively.

4.2.3 Third Module

The third module behaved as expected. The voltage decreased and the current increased as the resistance was decreased (Fig. 4.8) for a temperature difference of $60^{\circ}\text{C} \pm 1^{\circ}\text{C}$. The V-I curve was linear and the power curve seemed to follow a parabolic curve (Fig. 4.9). The power doesn't go as low on the right side of the maximum as the second module's does because of the change in setup. The voltage measurement was now taken across the decade box and the ammeter instead of just

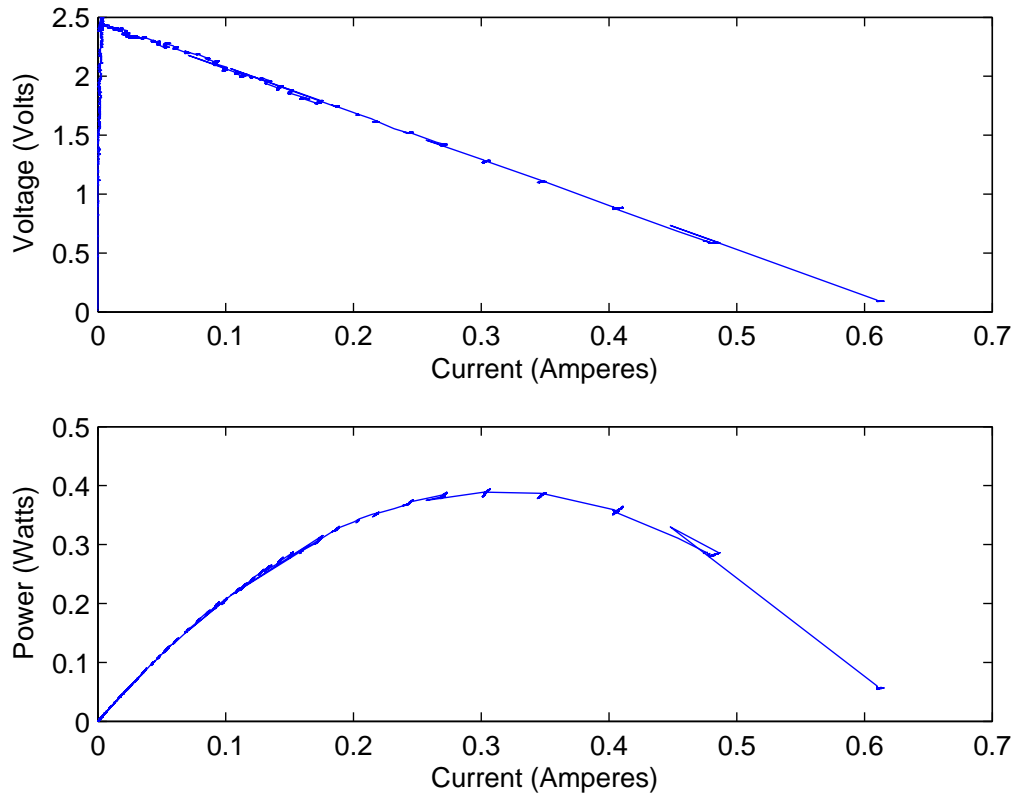


Figure 4.7 The I-V and power curves of the second module tested at a $60^{\circ}\text{C} \pm 1^{\circ}\text{C}$ temperature difference. The I-V curve is linear, which describes how the module will behave in a circuit. The power curve is parabolic, peaking at $394 \text{ mW} \pm 7 \text{ mW}$. The error in current and voltage measurements were $\pm 0.005 \text{ A}$ and $\pm 0.005 \text{ V}$, respectively.

the decade box. Since the ammeter has an internal resistance of $1.00 \Omega \pm 0.01 \Omega$, the resistance across the voltmeter could not get down to zero as it could in the old setup. The power curve peaks at $463 \text{ mW} \pm 6 \text{ mW}$ for a $60^{\circ}\text{C} \pm 1^{\circ}\text{C}$ temperature difference.

The error for raw current and voltage measurements for both modules were $\pm 0.005 \text{ A}$ and $\pm 0.005 \text{ V}$, respectively. These errors were due to the precision of the

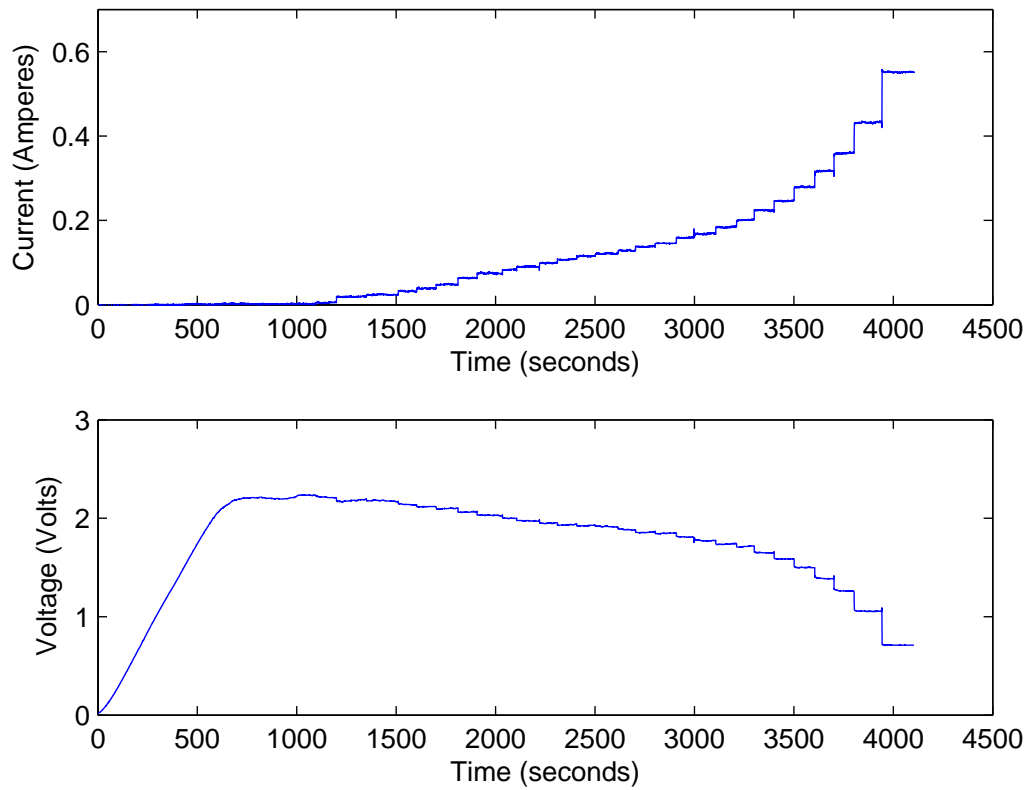


Figure 4.8 The voltage and current against time of the third module tested at a $60^{\circ}\text{C} \pm 1^{\circ}\text{C}$ temperature difference. As the resistance is lowered over time, the current increases and the voltage decreases, as expected. The error in current and voltage measurements were ± 0.005 A and ± 0.005 V, respectively.

instruments used.

4.3 Analysis

4.3.1 Second Module

The first module was not analyzed further as it was found to be damaged. The data from the second module was used to find out how the maximum power output changed

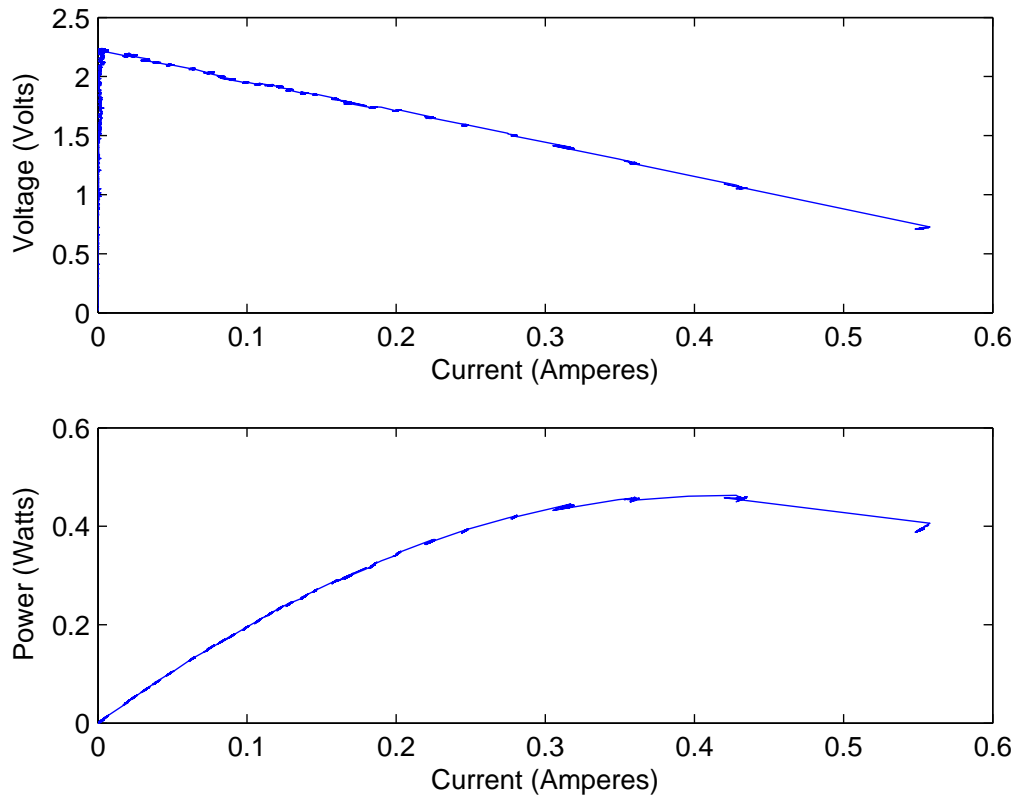


Figure 4.9 The power curves of the third module tested at a $60\text{ }^{\circ}\text{C} \pm 1\text{ }^{\circ}\text{C}$ temperature difference. The I-V curve is linear, which describes how the module will behave in a circuit. The power curve is parabolic, peaking at $463\text{ mW} \pm 6\text{ mW}$. The error in current and voltage measurements were $\pm 0.005\text{ A}$ and $\pm 0.005\text{ V}$, respectively.

with temperature. As seen in Fig. 4.10, the maximum power output increases with increasing temperature difference. The relationship appears to be quadratic, which would agree with Eq. 2.7. There are not enough data points, or a great enough temperature range, to definitely claim this.

The data from the second module was used in Eq. 2.9 to find the internal resistance of the module at various temperature differences. As seen in Fig. 4.11, the internal resistance does change with temperature difference, but it does not follow

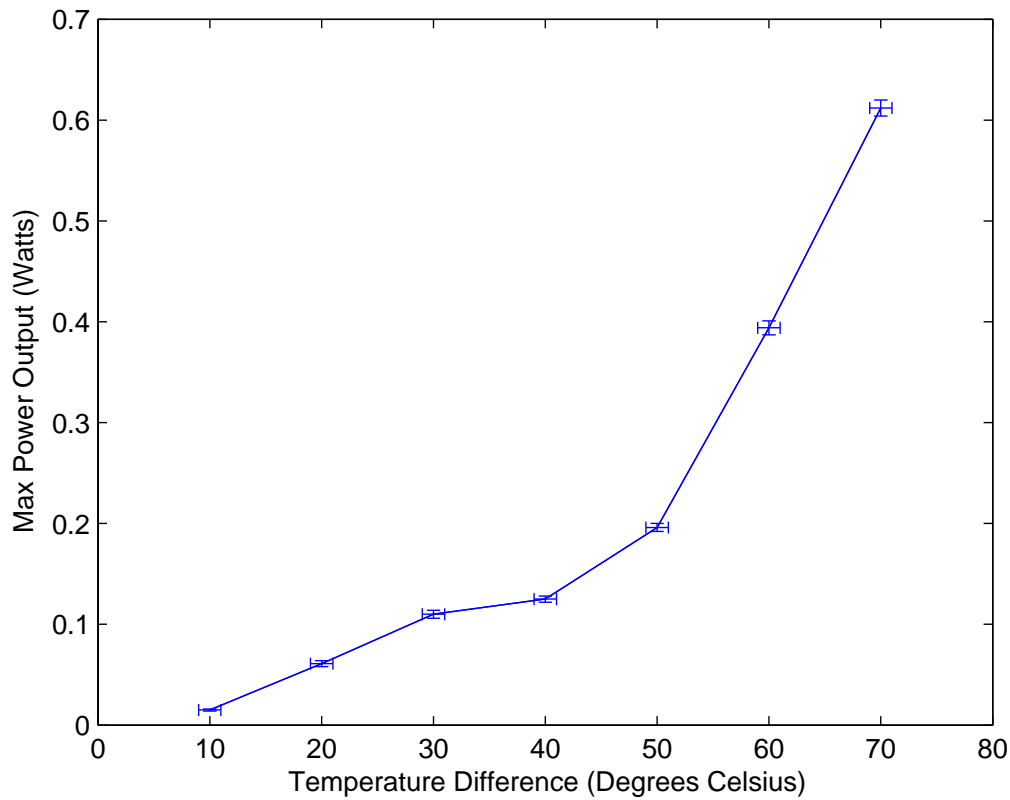


Figure 4.10 The maximum power output of the second module for various temperature differences. The power output increases with increasing temperature difference, which is expected.

any trend. According to the Hi-Z website, the internal resistance should increase with increasing temperature difference [18]. I suspect that the reason that this module's resistance does not steadily increase is due to the poor connectivity of the leads that was mentioned earlier.

4.3.2 Third Module

The maximum power outputs for each temperature difference were also plotted for the third module in Fig. 4.12. The power increases as the temperature difference

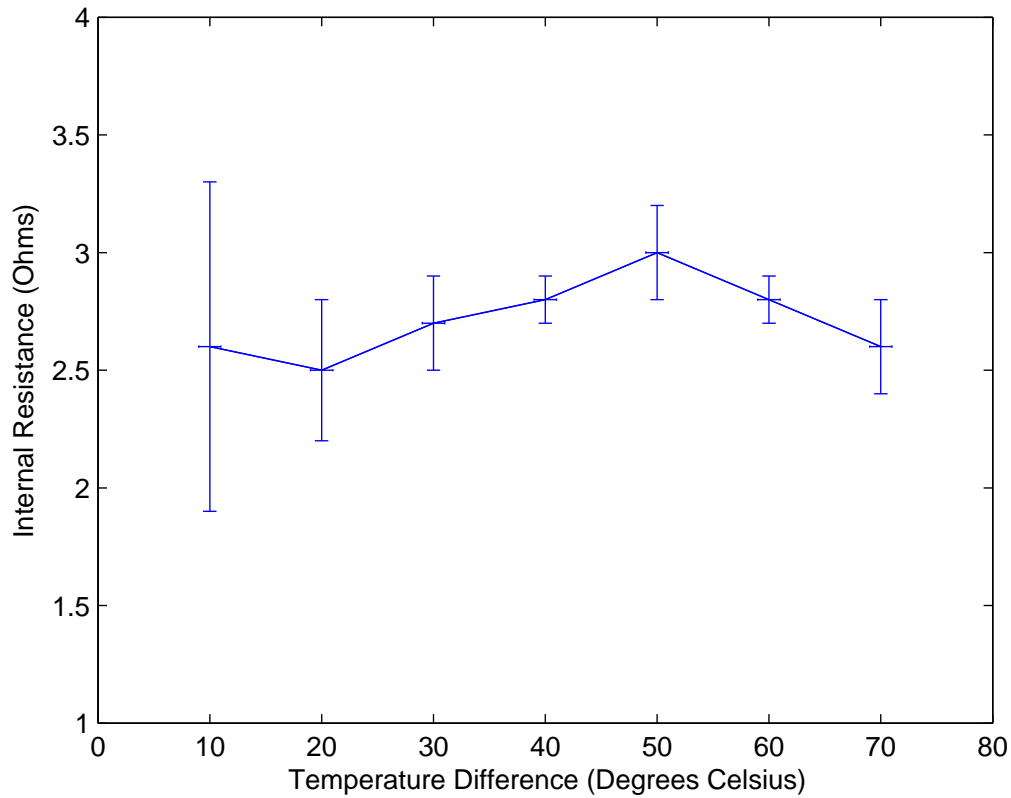


Figure 4.11 The graph of internal resistance of the second module for various temperatures. The internal resistance does not follow any consistent trend as temperature increases.

increases, as was seen in the second module. The curve again looks like it may be quadratic. The curve looks slightly different from the curve of the second module. This is not only due to the damage of the second module, but also to the change in circuit setup discussed previously. The measured power output of the second module was a measurement of the system of the module and ammeter in series, not just the module by itself. This affects the results, although it is difficult to see the extent by simply comparing the graphs due to the possible additional effect of the damage.

The internal resistance of the third module was plotted against changing tempera-

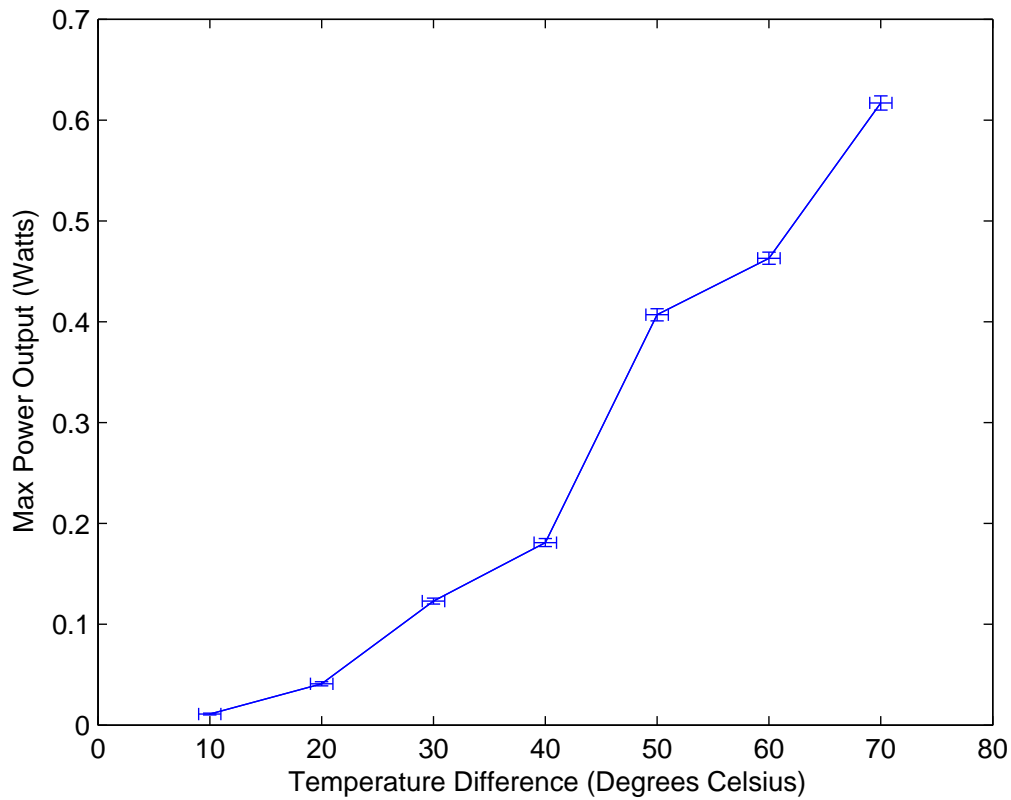


Figure 4.12 The maximum power output of the third module for various temperature differences. The power output increases with increasing temperature difference, which is expected.

ture difference in Fig. 4.13. For this module, the internal resistance steadily increased with increasing temperature difference. This agrees with Hi-Z's website [18], suggesting that it was in fact the damage that caused the second module's internal resistance to not have a consistent trend. Since the third module was brand new and had no visible damage, it behaved as predicted.

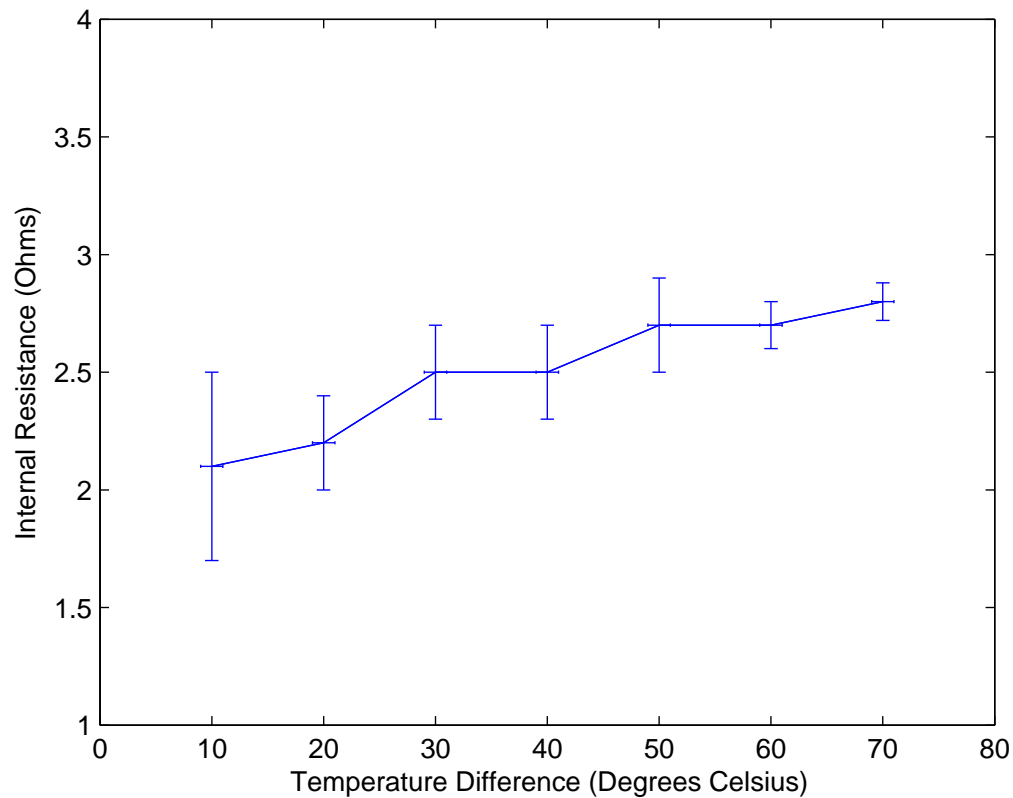


Figure 4.13 The graph of internal resistance of the third module for various temperatures. The internal resistance of this module increases as temperature increases. Since the resistance of semiconductors typically decreases with increasing temperature, the metal components of the module seem to have more of an effect on the resistance than the semiconductors.

4.3.3 Error

The error for temperature difference for was $\pm 1^\circ\text{C}$, which was the range between which I was able to keep the module by adjusting the hot plate and stirring the ice water. The error for power was found using the following equation, derived from the general formula for error propagation [19] and Eq. 2.8.

$$\delta P = P \sqrt{\left(\frac{0.005}{V}\right)^2 + \left(\frac{0.005}{I}\right)^2} \quad (4.2)$$

The error for internal resistance was found using the following equation, also derived from the general formula for error propagation [19] along with Eq. 2.9.

$$\delta R_{int} = \sqrt{\left(\frac{\delta V_{OC}}{I_L}\right)^2 + \left(\frac{-V_{OC}}{I_L^2} \delta I_L\right)^2 + (\delta R_L)^2} \quad (4.3)$$

4.4 Discussion

The ideal temperature difference of $60^\circ\text{C} \pm 1^\circ\text{C}$ produces a maximum power output of $463 \text{ mW} \pm 6 \text{ mW}$ from one module. By comparison, a standard four-battery NiMH battery charger consumes between 4 W and 5 W when charging all four batteries. Obviously, charging less batteries would require less power. Since power is energy per time, one thermoelectric module would still be able to charge the four batteries, but it would work much slower than a commercial battery charger. In order to charge batteries in a reasonable amount of time, more modules will need to be used in series, or a larger module will need to be used. Both of these options would increase the power output.

Since maximum power output increases with increasing temperature difference, it is desired that the module be kept between the greatest temperature difference possible. This is why, as discussed previously, it is important to transfer the most amount of energy possible from the center of the compost pile to the outside, where the module will be.

The fact that the internal resistance of a thermoelectric module increases with increasing temperature is surprising. The modules are made from bismuth telluride based semiconductors. In general, the resistance of semiconductors decreases with

increasing temperature, but here the opposite is seen. Since the resistance of most metals increases with increasing temperature, this suggests that the metals in the module affect its resistance more than the semiconductors.

Chapter 5

Conclusions

5.1 Can We Charge Batteries With Compost?

It had been found previously in lab replications that it is possible to charge batteries using the waste energy from a compost pile using thermoelectric modules. In this project, ways of improving the efficiency of this process were explored. The use of a copper slab insulated with extruded polystyrene would transfer $86\% \pm 2\%$ from the center of a pile, where it is the hottest, to the outside, where a charger would be. This is a significant percentage, but a larger percentage is desired because a large temperature difference across the module means a larger power output.

The power output of a module increases with increasing temperature, and at a $60\text{ }^\circ\text{C} \pm 1\text{ }^\circ\text{C}$ temperature difference one undamaged module can produce $463\text{ mW} \pm 6\text{ mW}$ at matched load. This amount of power is able to charge a battery slowly, but more modules or a bigger module would be needed for faster charging.

The internal resistance of a thermoelectric module is not constant; it increases with increasing temperature, probably due to the metal components having more of an effect on the module's resistance than the semiconductors. In order for a ther-

moelectric battery charger to be as efficient as possible, it needs to be built with technology that tracks the internal resistance and adjusts with temperature fluctuations for maximum power output.

Building a compost-powered battery charger is definitely possible. More work is needed to develop a finished product that will be as efficient as possible. This product is a step toward more renewable energy and away from dirty, finite fossil fuels. This device also encourages the sustainable practice of composting.

5.2 Future Work

There is still much more work to be done on this project. Better ways of transferring energy from the center of the pile to the outside should be investigated. Ultimately, a functioning battery charger should be built that uses one or more thermoelectric modules and takes advantage of maximum power point tracking technology. All the testing done in this thesis was with one module. Testing for power output and internal resistance needs to be done for multiple modules in series or with larger modules to see how the power output changes.

Other sources of waste heat energy should be explored. Refrigerators, cars, and computers all generate waste energy that could be exploited. If a device was developed that could be compatible with multiple sources, it would be a marketable item that could save a large amount of energy.

Bibliography

- [1] U. Bardi, "Peak Oil: The four stages of a new idea," *Energy*, **34** 323-326 (2009).
- [2] L. R. Brown, *Plan B 3.0: Mobilizing to Save Civilization*, (W. W. Norton & Company, New York, 2008).
- [3] V. P. Zhdanov, "Coarse-grained model of long-term supply of oil," *Eur. Phys. J. B.*, **71** 289-292 (2009).
- [4] P. Hanlon, and G. McCartney, "Peak Oil: Will it be public health's greatest challenge?" *Public Health*, **122** (7) 647-652 (2008).
- [5] US Department of Energy, Fossil Fuels website, <http://www.energy.gov/energysources/fossilfuels.htm> (Accessed February 26, 2010).
- [6] C. Howard, (2009) *Compost Thermal Heating Project*. Senior thesis. Ithaca College, Ithaca, New York. *Power Delivery*, **Vol 1** 186-191 (1995).
- [7] C. Yu, and K. T. Chau, "Thermoelectric automotive waste heat energy recovery using maximum power point tracking," *Energy Conservation and Management*, **50**(6) 1506-1512 (2009).
- [8] K. Qiu, and A. C. S. Hayden, "Development of a thermoelectric self-powered residential heating system," *Journal of Power Sources*, **180** 884-889 (2008).

- [9] M. Rahman, and R. Shuttleworth, "Thermoelectric power generation for battery charging," Proceedings of the International Conference on Energy Management and and
- [10] J. Eakburanawat, and I. Boonyaroonate, "Development of thermoelectric battery-charger with microcontroller-based maximum power point tracking technique," Applied Energy, **83** 687-704 (2006).
- [11] J. A. Edminister, *Shaum's Outline of Electric Circuits*, 2nd Ed. (McGraw-Hill, New York, 1994), 32.
- [12] Cornell Waste Management Institute, Cornell Composting website, http://compost.css.cornell.edu/Composting_Homepage.html (Accessed May 28, 2009).
- [13] Photo credit: City of Pierre website, <http://ci.pierre.sd.us/viewarticle.aspx?id=12&aid=75> (Accessed May 1, 2010).
- [14] D. Linden, and T. B. Reddy, *Handbook of Batteries*, 3rd Ed. (McGraw-Hill, New York, 2002).
- D. M. Rowe, and G. Min, "Design theory of thermoelectric modules for electrical power generation," IEE Proc-Sci Meas Technol, **143(6)** 351-356 (1996).
- G. J. Snyder, and T. S. Ursell, "Thermoelectric Efficiency and Compatibility," Physical Review Letters, **91(14)** 148301-1 - 148301-4 (2003).
- [15] Z. H. Dughaish, "Lead Telluride as a thermoelectric material for thermoelectric power generation," Physica B, **322** 205-223 (2002).
- [16] Picture credit: Peltier Device Information Directory, <http://www.peltier-info.com/> (Accessed June 23, 2009).

-
- [17] F. A. Leavitt, N. B. Elsner, and J. C. Bass, "Use, application, and testing of Hi-Z thermoelectric modules," Hi-Z Technology, Inc., <http://www.hi-z.com/>.
- [18] Hi-Z Technology, Inc., <http://www.hi-z.com/> (Accessed March 30, 2010).
- [19] J. R. Taylor, *An Introduction to Error Analysis*, 2nd Ed. (University Science Books, Sausalito, CA, 1997), Eq. 3.47.

